Spin polarization of tunneling current in barriers with spin–orbit coupling

2008 J. Phys.: Condens. Matter 20 115206

(http://iopscience.iop.org/0953-8984/20/11/115206)

J. Phys.: Condens. Matter **20** (2008) 115206 (6pp) doi:10.1088/0953-8984/20/11/115206

Spin polarization of tunneling current in barriers with spin–orbit coupling

T Fujita[1,2], M B A Jalil[1] and S G Tan[2]

[1] Information Storage Materials Laboratory, Electrical and Computer Engineering Department, National University of Singapore, 4 Engineering Drive 3, 117576, Singapore
[2] Data Storage Institute, DSI Building, 5 Engineering Drive 1, (off Kent Ridge Crescent, National University of Singapore), 117608, Singapore

Received 10 October 2007, in final form 15 January 2008
Published 20 February 2008
Online at stacks.iop.org/JPhysCM/20/115206

Abstract
We present a general method for evaluating the maximum transmitted spin polarization and optimal spin axis for an arbitrary spin–orbit coupling (SOC) barrier system, in which the spins lie in the azimuthal plane and finite spin polarization is achieved by wavevector filtering of electrons. Besides momentum filtering, another prerequisite for finite spin polarization is asymmetric occupation or transmission probabilities of the eigenstates of the SOC Hamiltonian. This is achieved most efficiently by resonant tunneling through multiple SOC barriers. We apply our analysis to common SOC mechanisms in semiconductors: pure bulk Dresselhaus SOC, heterostructures with mixed Dresselhaus and Rashba SOC and strain-induced SOC. In particular, we find that the interplay between Dresselhaus and Rashba SOC effects can yield several advantageous features for spin filter and spin injector functions, such as increased robustness to wavevector spread of electrons.

(Some figures in this article are in colour only in the electronic version)

1. Introduction

The production of spin-polarized current in semiconductors (SC) is an important but challenging step in the field of spintronics, in which electron transport is controlled based on the spin degree of freedom [1–3]. The long spin relaxation time observed in semiconductors [4–7], and the compatibility of this technology with current nanofabrication methods [8] makes semiconductor-based spintronics both an attractive and a viable avenue for future applications. Several techniques for creating spin current in semiconductors have been proposed such as direct injection of current from ferromagnetic (FM) metals. However, the large mismatch of conductivities of the two materials [9], and the depolarizing effects due to defects at the FM–SC interface [10] drastically reduce the efficiency of this process. A possible method of overcoming the conductivity mismatch is by utilizing diluted magnetic semiconductors (DMS) as spin injectors instead of FM metals. However, this faces the separate problem of low Curie temperature, which characterizes currently known DMS materials.

An alternative is to utilize spin–orbit coupling (SOC), an effect described by Dirac's equation in the non-relativistic limit, to directly induce spin-polarized current in semiconductors. Essentially, electrons traveling with momentum $\vec{k}$ in the presence of an electric field $\vec{E}$ feel an effective magnetic field along $\vec{k} \times \vec{E}$ which spontaneously breaks the spin degeneracy into two subbands. Previous works [11, 12] have theoretically demonstrated ways to preferentially filter one subband over the other, using techniques such as resonant tunneling with multiple barriers. However, because of the time-reversal (TR) invariance of SOC, these schemes still result in zero net spin polarization. In this paper, we propose to induce a finite spin polarization in a TR symmetric system via filtering of electrons in momentum or k-space. In particular, we theoretically analyze the spin polarization for arbitrary *azimuthal anisotropies* in k-space, and determine the reference axis along which the polarization is maximal. We first present the general derivation for these two quantities, that is valid for arbitrary spin–orbit systems with in-plane spins. Subsequently, we apply the results to three common SOC systems: (a) bulk k^3-Dresselhaus SOC, (b) combined linear-k Dresselhaus and Rashba SOC in two-dimensional heterostructures, and (c) strain-induced SOC.

2. Theory

We begin by considering the general spin–orbit Hamiltonian, obtained in the non-relativistic limit of the Dirac equation,

$$\mathcal{H}_{\rm SO} = -\frac{\hbar^2}{4m^2c^2}\vec{\sigma}\cdot(\vec{k}\times\nabla V) \equiv -\lambda\vec{\sigma}\cdot\vec{\Omega}(\vec{k}), \tag{1}$$

where λ is the coupling parameter, $\vec{\sigma}$ is the vector of Pauli matrices, and $\vec{\Omega}(\vec{k})$ is a momentum-dependent effective magnetic field. The SOC spontaneously breaks the spin degeneracy into two subbands ($\pm$), separated by a spin split in energy of $2\lambda|\vec{\Omega}(\vec{k})|$. We denote the spin-split eigenstates (subbands) by spinors $\vec{\xi}_+$ and $\vec{\xi}_-$. The two eigenstates consist of an ensemble of degenerate electron modes $\vec{k}$, whose spins lie either parallel (+) or antiparallel (−) to the effective field, $\vec{\Omega}(\vec{k})$. Due to TR symmetry, the effective field satisfies $\vec{\Omega}(\vec{k}) = -\vec{\Omega}(-\vec{k})$ within each band. Thus, if transport occurs across the entire Fermi surface, the net spin polarization of current in a SOC system must necessarily vanish. In order to induce a finite spin polarization, one must explicitly break the TR symmetry e.g. by introducing an external magnetic field, or incorporating magnetic moments. Alternatively, one may measure a finite spin polarization by selecting and analyzing electrons with certain momenta.

We consider a selective filtering of electrons in the azimuthal k-space, i.e. in $\vec{k}_\parallel = (k_x, k_y)$. To quantify the spin polarization in the system, we first consider a reference spin axis γ, and compute the *transmitted spin conductance* along this axis, i.e. the conductance of electrons with spins polarized along γ. Our objective is to determine the optimum axis, $\gamma_{\rm opt}$, along which the spin conductance is a maximum for a given filtering scheme. The transmitted spin conductance is defined as the product of the electron spin S along γ, and the particle conductance, g_z. Following the density matrix formalism [13], the expectation value of the transmitted spin conductance for arbitrary azimuthal γ is

$$\langle g_z S_\gamma\rangle = {\rm Tr}(\rho g_z S_\gamma), \tag{2}$$

where g_z is the particle conductance per transmitted mode, and S_γ is the spin projection operator along γ, $S_\gamma = S_x\cos\gamma + S_y\sin\gamma$ [14]. We assume a maximum particle conductance of $g_z = e/h$ (NB the maximum ballistic charge conductance is e^2/h per mode). Note that equation (2) is effectively a measure of the spin polarization along γ. The density matrix ρ in equation (2) describes the mixed state of eigenstates in the system [13–15], and is given by $\rho = P_+|\vec{\xi}_+\rangle\langle\vec{\xi}_+| + P_-|\vec{\xi}_-\rangle\langle\vec{\xi}_-|$, where $P_+(P_-)$ is the probability of an electron being in eigenstate +(−). Since the intrinsic angular momentum associated with an electron spin is $\hbar/2$, the maximum spin conductance per transmission mode is given by $g_z S = (e/h)(\hbar/2) = e/4\pi$. Until now, the analysis has been completely general. For illustrative purposes, we focus now on SOC systems whose spins are in-plane (i.e. the SO Hamiltonian contains only the σ_x and σ_y Pauli matrices), as many common SOC systems are of this type. For these SOC systems, the eigenspinors have the general form of

$$\vec{\xi}_\pm = (\pm {\rm e}^{{\rm i}\chi(\vec{k})}, 1)^{\rm T}/\sqrt{2}, \tag{3}$$

where $\chi(\vec{k})$ is a momentum-dependent phase factor, and the $\pm$ indexes the two spin-split subbands. Expanding equation (2), one then obtains

$$\langle g_z S_\gamma\rangle = \frac{e}{4\pi}(P_+ - P_-)\cos(\gamma + \chi(\phi)), \tag{4}$$

where $\phi = \arctan(k_y/k_x)$. $(P_+ - P_-) \equiv \eta$ is the *subband filtering efficiency*, which measures the efficiency of preferentially selecting one eigenstate (subband) over the other, and its value depends on the particular method used to filter the spin eigenstates. There are a number of ways of achieving this, which we shall discuss later. To obtain the total spin conductance due to all modes, equation (4) must be integrated in k-space over the contributing portion of the Fermi surface. If there are no constraints in k-space, then the integration covers all modes on the Fermi surface (i.e. ϕ goes from 0 to 2π), which yields zero spin conductance for any γ, regardless of whether $\eta \neq 0$. In order to achieve a finite polarization, we limit the k-space distribution of electrons to *part* of the Fermi surface. For simplicity, we consider a filtering scheme such that transmission is allowed only for electron modes with wavevectors $\vec{k}_\parallel = (k_x, k_y)$ pointing in some range of azimuthal angle $\phi \in (\phi_1, \phi_2)$. Under this scheme, the spin polarization along a given γ is averaged over the collected modes:

$$\mathcal{P}_\gamma = \frac{1}{\Delta\phi}\int_{\phi_1}^{\phi_2}\eta(\phi)\cos(\gamma + \chi(\phi))\,{\rm d}\phi, \tag{5}$$

where $\Delta\phi = \phi_2 - \phi_1$. When $P_\pm$ and hence η is independent of ϕ (as is the case for the systems studied in the next section), we find that for a collection range of $\phi \in (\phi_1, \phi_2)$, the optimal spin axis which yields maximum spin polarization $\mathcal{P}_\gamma$ is given by

$$\gamma_{\rm opt} = -\arctan\left(\frac{\int_{\phi_1}^{\phi_2}\sin\chi(\phi)\,{\rm d}\phi}{\int_{\phi_1}^{\phi_2}\cos\chi(\phi)\,{\rm d}\phi}\right). \tag{6}$$

Since k-space filtering is a prerequisite for achieving finite spin polarization in an SOC system, we will briefly discuss how it may be achieved in practice. A possible method is to implement a collector that preferentially collects electrons with a certain wavevector distribution. For example, following Koga *et al* [12] and Ting *et al* [16], one can preferentially select electrons with $k_x > 0$ by placing a collector along the positive $\hat{x}$-direction (with respect to the center coordinate of the sample). Strictly, such a one-sided collector will break the translational symmetry in the $\hat{x}$-direction, so that $k_\parallel$ can no longer be regarded as a good quantum number. However, following [12, 16], we assume that the collector is sufficiently decoupled from the central SOC region, so that $k_\parallel$ is still well defined within the SOC region. Suppose we have a sample with longitudinal dimension (of say L, along $\hat{z}$) of the order of the mean free path, so that the electron transport is ballistic. An electron injected from one end of the sample with transverse momenta $\vec{k}_\parallel = (k_x, k_y)$, would therefore leave the sample with the same $\vec{k}_\parallel$. For an electron with $k_x > 0$, we therefore require that the transverse shift along $\hat{x}$ of the electron be at least $L_x/2$, where L_x is the length of the sample along the $\hat{x}$-direction, i.e. we require

$$v_x t > \frac{L_x}{2} \tag{7}$$

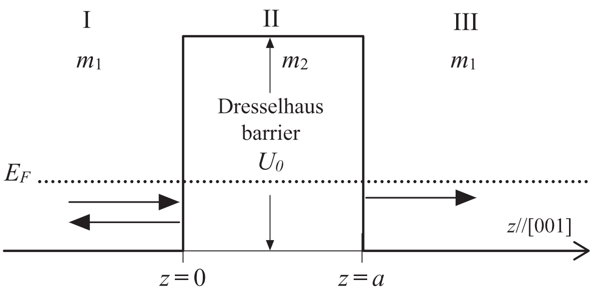

Figure 1. The spin-dependent tunneling process, where the barrier exhibits bulk-inversion asymmetry. Under Dresselhaus spin–orbit coupling, electrons are transmitted into region III with different probabilities P_+, P_- depending on their spin state.

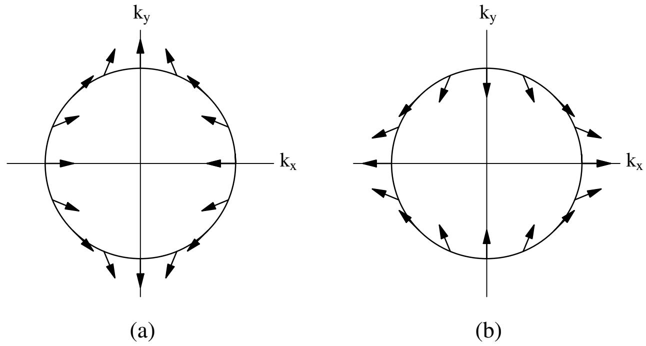

Figure 2. Spin orientations in the xy-plane, along the Fermi circle for electrons in (a) '+' eigenstate, and (b) '−' eigenstate under spin–orbit coupling induced by bulk-inversion asymmetry (BIA).

where $v_x = \hbar k_x/m^*$ is the electron's $\hat{x}$-velocity and $t = L/v_F$ is the time of transport of the electron through the sample (v_F is the Fermi velocity). In an alternative scheme, one could induce an asymmetry in the transverse electron momentum distribution by applying a small electric field in the transverse direction [17].

In the following section, we will apply the above general analysis to several specific SOC systems.

3. Applications—results and discussion

3.1. Spin-dependent tunneling through semiconductors with bulk-inversion asymmetry

We first consider the spin polarization of the tunneling electrons across a semiconductor (SC) barrier with a bulk-inversion asymmetry (BIA) in its crystal lattice. Such a crystal structure (e.g. zincblende structure) exhibits k^3-Dresselhaus SOC. We assume the barrier has width a along the $\hat{z}$-direction, which corresponds to the crystal [001] axis. The barrier potential profile is represented by a square hat function $U(z) = U_0[\Theta(z) - \Theta(z-a)]$, as shown in figure 1. In the presence of Dresselhaus SOC, the Hamiltonian which describes electron transport in the SC barrier is [11]

$$\mathcal{H} = \frac{\vec{p}^2}{2m^*} - \beta(k_y\sigma_y - k_x\sigma_x)\nabla_z^2 + U(z), \tag{8}$$

where $\vec{p}$ is the electron momentum, m^* is the effective mass of electrons, β is the Dresselhaus parameter (in eV m^3), and σ_i are the Pauli spin matrices. The eigenspinor solutions to equation (8) are

$$\vec{\xi}_\pm = \frac{1}{\sqrt{2}}\begin{pmatrix} -\frac{s(k_x+\mathrm{i}k_y)}{k_\parallel} \\ 1 \end{pmatrix} = \frac{1}{\sqrt{2}}\begin{pmatrix} -s\exp(\mathrm{i}\phi) \\ 1 \end{pmatrix}, \tag{9}$$

where $s = \pm 1$ correspond to the two spin eigenstates, and $k_\parallel = (k_x^2 + k_y^2)^{\frac{1}{2}}$ is the in-plane wavevector magnitude. Each eigenstate consists of an ensemble of electrons whose spins are oriented in the xy-plane, as illustrated in figure 2. The solutions to the Schrödinger equation $\mathcal{H}\Psi_\pm(x,y,z) = E_\pm\Psi_\pm(x,y,z)$ are of the form $\Psi_\pm(x,y,z) = \vec{\xi}_\pm\psi_\pm(z)\exp(\mathrm{i}k_x x + \mathrm{i}k_y y)$ where $\psi_\pm(z)$ are the traveling wave components. In particular, the traveling component in region III (see figure 1) is

$$\psi_\pm^{\mathrm{III}}(z) = t_\pm \exp(\mathrm{i}k_z z), \tag{10}$$

where $t_\pm$ are the transmission coefficients. These are obtained by performing wavefunction and flux matching at the region boundaries:

$$t_\pm = \frac{-2K_1K_2k_zq_\pm}{\mathrm{i}\left(q_\pm^2K_2^2 + k_z^2K_1^2\right)\sin(q_\pm a) - 2K_1K_2k_zq_\pm\cos(q_\pm a)}, \tag{11}$$

where $K_1 = \hbar^2/2m_1$, $K_2 = \hbar^2/2m_2 \pm \beta k_\parallel$ and q (k_z) is the wavevector inside (outside) of the barrier, given by

$$q_\pm = \left(\frac{\frac{2m_2}{\hbar^2}(E_F - U_0) - k_\parallel^2}{1 \pm \frac{2m_2}{\hbar^2}\beta k_\parallel}\right)^{\frac{1}{2}}, \qquad k_z = \left(\frac{2m_1}{\hbar^2}E_F - k_\parallel^2\right)^{\frac{1}{2}}. \tag{12}$$

In the above, E_F is the Fermi energy, and m_1, m_2 are the effective masses outside (RI and RIII), and within (RII) the SC barrier, respectively. The transmitted spin conductance is obtained by applying equation (4) and substituting

$$P_\pm = \frac{|t_\pm|^2}{|t_+|^2 + |t_-|^2}, \tag{13}$$

which denote the probabilities of $\pm$ eigenstate occupation in RIII. Since $P_\pm$ are independent of ϕ, we can evaluate the optimum spin axis using equation (6). This yields a surprisingly simple result of

$$\gamma_{\mathrm{opt}} = -\frac{\phi_1 + \phi_2 + 2\pi}{2}, \tag{14}$$

for the optimal spin axis, along which the spin polarization is maximized,

$$\mathcal{P}_{\max} = \frac{2\eta}{\Delta\phi}\sin\left(\frac{\Delta\phi}{2}\right) = \eta f(\Delta\phi). \tag{15}$$

Equation (15) shows that the net spin polarization is given by the subband filtering efficiency η scaled by the factor $f(\Delta\phi)$, which describes the effect of averaging over modes $\Delta\phi$ on the spin polarization. Since $f(\Delta\phi)$ is a monotonically decreasing function over the range $0 \leqslant \Delta\phi \leqslant 2\pi$, averaging over a wider angular spread of transmission modes will inevitably result in a lower spin polarization. We performed numerical calculations for barriers made of semiconductor materials which exhibit BIA, e.g. GaAs, GaSb and InSb. We assumed the following parameters for (GaAs, GaSb and InSb) [11, 18]: $m^*/m_0 = (0.067, 0.041, \text{and } 0.013)$, and $\beta = (24, 187, \text{and } 220)$ eV Å^3. We also set $E_F = 20$ meV corresponding to typical carrier densities of 10^{16}–10^{17} cm^{-3} [19], $k_\parallel = 2.5 \times 10^8$ m^{-1}, and assumed a barrier of height $U_0 = 70$ meV and width 2.7 nm. The chosen width allows us to achieve an appreciable spin polarization and tunneling current magnitude. In figure 3 we plot the maximum spin polarization for the different barrier materials with increasing collection span $\Delta\phi = \phi_2$ (with $\phi_1 = 0$ fixed). Clearly, the highest spin polarization corresponds to collection of only a single transmission mode for each eigenspinor (i.e. $\Delta\phi \to 0$). Any angular spread $\Delta\phi$ in the collection process, which inevitably occurs in practice (e.g. due to the inherent spread in the incident electrons, or $k_\parallel$-mixing type of scattering events within the SOC region), will cause a reduction in the spin polarization. As noted previously the spin polarization ultimately vanishes when $\Delta\phi = 2\pi$. In figure 3 we also plot the optimal orientation of the reference spin axis γ_{opt} of the detector in region III. The variation of γ_{opt} with $\Delta\phi$ means that it is necessary to have a collector with a tunable spin or magnetization axis in order to harness the maximum spin polarization of the transmitted current. Note that the spin polarization achievable in this tunneling scheme is only of the order of 1%. This is because the maximum polarization is constrained by the subband selectivity ratio η, which is relatively low in the present tunneling scheme. To achieve a higher spin polarization, we require a system with a much higher subband filtering efficiency. One such system is a multi-barrier structure with SOC effect, which exhibits resonant spin-dependent tunneling, as discussed in the following section.

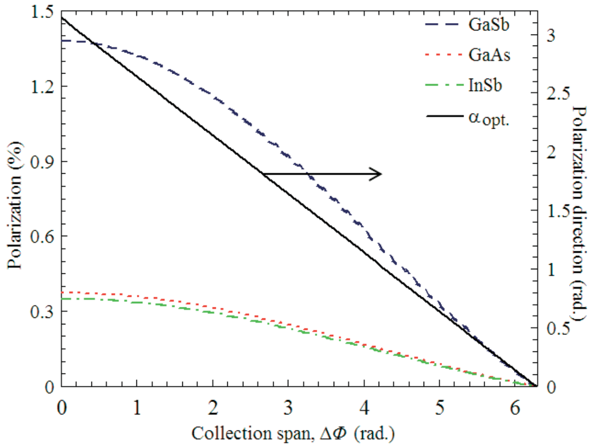

Figure 3. Maximum spin polarization for electrons tunneling through a bulk k^3-Dresselhaus barrier, under k-space filtering, such that only electrons traveling in the azimuthal direction $\phi = \arctan k_y/k_x \in (0, \Delta\phi)$ are collected. A broader momentum collection distribution (i.e. larger $\Delta\phi$) leads to a reduced spin polarization, which ultimately vanishes when the entire Fermi circle is collected. Superimposed is the corresponding (azimuthal) net spin polarization direction.

3.2. Spin polarization in heterostructures induced via resonant tunneling

Recently, there has been a wealth of theoretical study on resonant tunneling structures which utilize the SOC in heterostructures to achieve an extremely high (near perfect) subband filtering performance [12, 20]. In such two-dimensional heterostructures, the dominant intrinsic SOC mechanisms are the Rashba and linear-k Dresselhaus types, described by the Hamiltonian

$$\mathcal{H} = \frac{\vec{p}^2}{2m^*} + \alpha(\sigma_x k_y - \sigma_y k_x) + \beta(\sigma_x k_x - \sigma_y k_y), \qquad (16)$$

where α, β are the Rashba and Dresselhaus coupling strengths, respectively.

In the multi-barrier resonant tunneling structures, the SOC effects can induce a clear spin splitting of the transmission resonances, which results in a high subband selectivity. In [12], Koga *et al* proposed a non-magnetic, triple-barrier resonant tunneling diode (TB-RTD), where spin splitting between the resonant tunneling modes is induced under the influence of the Rashba SOC effect. With a sufficiently large spin splitting between the subband modes and by tuning the emitter–collector bias, transmission can be made to selectively occur in one of the subbands while being suppressed in the other. In this structure, the subband transmission probabilities are defined as

$$P_\pm = \frac{I_\pm}{I_+ + I_-}, \qquad (17)$$

where $I_\pm$ is the transmitted tunneling current of the $\pm$ subbands through the TB-RTD, which are given by the following integral up to the Fermi level [12, 16]:

$$I_\pm = \frac{|e|}{h} \int\int T_\pm(E, \vec{k}_\parallel)\,\mathrm{d}E\,\mathrm{d}\vec{k}_\parallel. \qquad (18)$$

Under optimal conditions, an extremely high subband filtering efficiency of $\eta = 99.9\%$ is predicted. In [12] only the Rashba SOC interaction was considered, in which case the eigenvalues, $E_\pm = \hbar^2k^2/2m^* \pm \alpha k_\parallel$, are isotropic in the azimuthal plane in k-space. Since the transmission probabilities $T_\pm$ and hence $P_\pm$ are then ϕ-independent, this case is similar to the bulk Dresselhaus system considered in the previous section, except for the much larger value of η. Thus, the optimal spin polarization axis is a linear function of ϕ_2 (with $\phi_1 = 0$), and the spin polarization has the same dependence on the collection span $f(\Delta\phi)$, as in equation (15).

Of greater interest is the case where both Rashba and linear Dresselhaus SOC effects are present in the system. The corresponding eigenvalues are $E_\pm = \hbar^2k^2/2m^* \pm \sqrt{\alpha^2 + \beta^2 + 2\alpha\beta\sin(2\phi)}k_\parallel$, while the eigenspinors $\xi_\pm$ are given by equation (3) with

$$\chi(\vec{k}) = \arctan\left(\frac{\alpha\cos\phi + \beta\sin\phi}{\alpha\sin\phi + \beta\cos\phi}\right). \qquad (19)$$

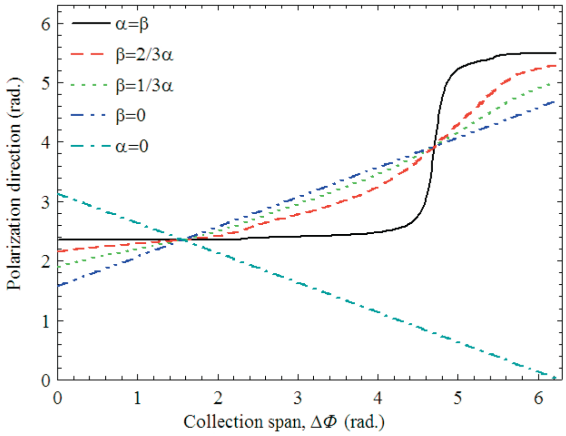

Figure 4. Net (azimuthal) spin polarization direction as a function of collection span, in the presence of combined Dresselhaus and Rashba SOC effects. The electrons are subject to k-space filtering, such that only those traveling in the azimuthal direction $\phi = \arctan k_y/k_x \in (0, \Delta\phi)$ are collected. For the Rashba-only ($\beta = 0$) and Dresselhaus-only ($\alpha = 0$) cases, the spin polarization has a linear dependence on the collection span $\Delta\phi$. The dependence becomes increasingly non-linear as the spin–orbit parameter ratio β/α approaches unity.

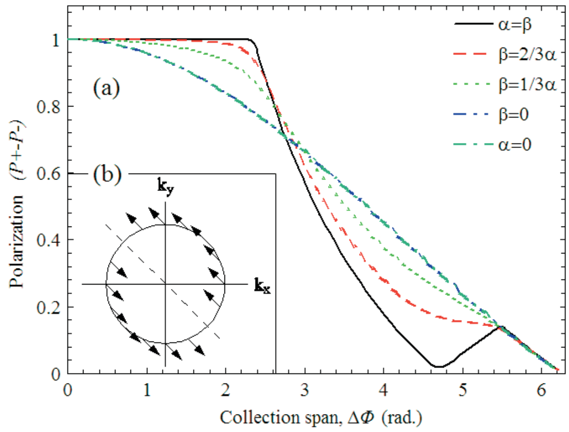

Figure 5. (a) Maximum spin polarization normalized to the subband filtering efficiency η as a function of collection span, of combined Dresselhaus and Rashba SOC effects. The electrons are subject to k-space filtering, such that only those traveling in the azimuthal direction $\phi = \arctan k_y/k_x \in (0, \Delta\phi)$ are collected. For the Rashba-only and Dresselhaus-only cases, the spin polarization behavior is identical to the k^3-Dresselhaus case in bulk (see figure 3). In contrast, for β/α tending to unity, the polarization behavior shows distinctive features such as a plateau of high spin polarization at small $\Delta\phi$, and non-monotonic behavior at large $\Delta\phi$ values. (b) The azimuthal spin orientation of electron modes in the + subband of the combined Rashba–Dresselhaus system, when $\alpha = \beta$. The shape of the polarization curve in (a) can be explained qualitatively when one considers the distributions of spins in k-space.

Since $E_\pm$ and $\vec{\xi}_\pm$ are anisotropic in the azimuthal plane, the transmission probabilities $T_\pm$ and hence the subband currents $I_\pm$ are now ϕ-dependent. However, we can simplify the transport analysis by assuming (following [16]) that $I_\pm$ are ϕ-*independent* even when $\beta \neq 0$. This isotropic approximation can be justified as follows [16]: $I_\pm$ are determined by integrating the transmission probabilities $T_\pm$ up to the Fermi energy E_F based on equation (18). Numerically it was found that the resonance peak strengths of $T_\pm$ are not strongly dependent on ϕ. Additionally, for typical values of E_F, the main peaks of $T_\pm(E)$ usually lie below E_F for all ϕ. Under these conditions, the integrated quantity $I_\pm$ will have a much weaker ϕ-dependence. With the isotropic approximation in hand, we apply equation (6) to determine the optimal spin reference axis γ_{opt}. The variation of γ_{opt} with the collection span $\Delta\phi$ (shown in figure 4) arises from the ϕ-dependence of the eigenspinors $\vec{\xi}_\pm$. The corresponding polarization $\mathcal{P}_{\gamma=\gamma_{opt}}$, normalized to $\eta \equiv (P_+ - P_-)$, is plotted in figure 5. Note that we have plotted the dependence of γ_{opt} and $\mathcal{P}_\gamma$ on $\Delta\phi$ for different ratios of Rashba to Dresselhaus SOC parameters, β/α, because the shape of the curves depends only on this ratio.

In the presence of Dresselhaus SOC only, i.e. $\alpha = 0$, we recover the linear variation of γ_{opt}, which is similar to the k^3-Dresselhaus SOC case studied in the previous section. At the other extreme, i.e. $\beta = 0$ (Rashba-only) case, γ_{opt} also shows a linear variation but with a gradient of opposite sign. This is because the effective field directions due to Rashba and Dresselhaus SOC effects are perpendicular to one another, as can be seen from equation (16). As for the $\Delta\phi$-dependence of the polarization $\mathcal{P}_\gamma$, both cases show identical behavior, i.e. monotonic decrease with collection span according to equation (15).

The more interesting case of mixed Dresselhaus and Rasbha SOC, i.e. for finite β/α values, show several qualitatively different behaviors in γ_{opt} and $\mathcal{P}_\gamma$. We highlight three distinctive features with potential practical utility: (a) γ_{opt} exhibits a non-linear variation as a function of $\Delta\phi$, as shown in figure 4. This is especially obvious if the two coupling constants are comparable, i.e. as $\beta/\alpha \to 1$. In fact, when $\beta/\alpha = 1$, γ_{opt} becomes relatively constant for a large range of $\Delta\phi$. This is advantageous from a practical standpoint since the reference axis of the collector can be fixed at e.g. $\gamma_{opt} = 3\pi/4$, regardless of the k-filtering scheme. (b) Another interesting feature is that when the collection span is set at the critical value of $\Delta\phi_0 = \pi/2$ or equivalently at $3\pi/2$, the optimal spin axis remains constant regardless of the relative values of α and β. This characteristic will be useful in a tunable spin filter device, in which the Rashba constant α can be changed relative to the Dresselhaus constant β by applying a gate bias which modifies the band structure at the interface of the heterostructure [12, 21]. If the k-filtering scheme is such that $\Delta\phi = \Delta\phi_0$, then the gate-bias-induced change of β/α ratio will only modify the filtering efficiency of the device (i.e. $\mathcal{P}_\gamma$), without affecting the orientation of the collected spin current. (c) Thirdly, we find that as β/α approaches unity, the normalized spin polarization $\mathcal{P}_\gamma$ becomes insensitive to an initial broadening of the wavevector collection spread $\Delta\phi$. As shown in figure 5, for $\beta/\alpha = 1$, $\mathcal{P}_\gamma$ is maintained almost at its maximum value of 1 for a sizable range of collection span of $0 \leqslant \Delta\phi \lesssim 3\pi/4 \approx 2.35$ rad before decreasing. Thus, one can potentially improve the robustness of the proposed spin filter/injector device to an angular spread of the wavevector of the incident electrons and $k_\parallel$-mixing due to scattering, by designing the heterostructure or tuning the gate bias, so that the Rashba and Dresselhaus SOC effects are of equal strength. This property also enables us to relax the strict requirement for 1D channel transport that is usually associated with devices based on SOC effects [22].

Finally, we note that when $\beta/\alpha \to 1$, the monotonically decreasing trend of the polarization curve no longer holds. As shown in figure 5, there is a small peak in the spin polarization curve, which is due to the particular symmetry of the eigenspinors for the $\alpha = \beta$ case (see inset (b) of figure 5). Unlike in the previous case with purely k^3-Dresselhaus SOC within the barrier, where a spread of electron momenta always reduces the transmitted spin polarization, we find that in the present system, the interplay between Rashba and Dresselhaus SOC can be utilized to counteract this averaging effect.

3.3. Strain-induced spin–orbit coupling

We end with a brief discussion of spin transport in strain-induced SOC systems. In general, the effective magnetic SO field $\vec{\Omega}(\vec{k})$ in equation (1) is permitted when there are broken inversion symmetries in the system. An example is the strain-induced asymmetry in bulk semiconductors. The most dominant form of such strain-induced SOC mechanism has the form [23, 24]

$$\mathcal{H} = D[k_x(\epsilon_{yy} - \epsilon_{zz})\sigma_x + k_y(\epsilon_{zz} - \epsilon_{xx})\sigma_y + k_z(\epsilon_{xx} - \epsilon_{yy})\sigma_z], \tag{20}$$

where D is a material-dependent parameter and ϵ_{ij} are elements of the strain tensor. If we consider a heterostructure with uniaxial strain characterized by $\epsilon_{xx} = \epsilon_{yy}$ [24], then equation (20) becomes

$$\mathcal{H} = -D\epsilon(k_x\sigma_x - k_y\sigma_y), \tag{21}$$

where $\epsilon = \epsilon_{zz} - \epsilon_{xx}$. Equation (21) has the same form as the Hamiltonian in equation (16) with the effective SOC constants of $\alpha = 0$ and $\beta = -D\epsilon$. Therefore, with these substitutions, the analysis of transmitted spin polarization in uniaxially strained SC follows in an identical fashion to that of the Rashba–Dresselhaus system presented earlier, but with the spin polarization direction rotated by π.

4. Conclusion

In conclusion, we have presented a general method for determining the optimal spin axis and maximum spin polarization, applicable to spin–orbit systems with in-plane spins and where time-reversal symmetry is broken by k-space filtering of the incident electrons. Another prerequisite for spin polarization is asymmetric transmission probabilities of the two subbands corresponding to the spin eigenstates of the SO Hamiltonian. This can be achieved best via resonant tunneling transport through multiple barriers. The general analysis is applied to several specific SOC systems: pure bulk Dresselhaus SOC, 2D heterostructure with mixed Dresselhaus and Rashba SOC effects and strain-induced SOC. We find that the interplay between Dresselhaus and Rashba SOC effects can yield several advantageous features for spin filter functions, such as increased robustness to wavevector spread of incident electrons.

Acknowledgments

The authors would like to thank the Agency for Science, Technology and Research (A*STAR) of Singapore, the National University of Singapore (NUS) Grant No. R-263-000-329-112 and the NUS Research Scholarship for financially supporting their work.

References

[1] Wolf S A, Awschalom D D, Buhrman R A, Daughton J M, von Molnar S, Roukes M L, Chtchelkanova A Y and Treger D M 2001 *Science* **294** 1488
[2] Žutić I, Fabian J and Sarma S D 2004 *Rev. Mod. Phys.* **76** 323
[3] Awschalom D D, Loss D and Samarth N (ed) 2002 *Semiconductor Spintronics and Quantum Computing* (Berlin: Springer)
[4] Kikkawa J M and Awschalom D D 1998 *Phys. Rev. Lett.* **80** 4313
[5] Feher G 1954 *Phys. Rev.* **114** 1219
[6] Kikkawa J M and Awschalom D D 1999 *Nature* **397** 139
[7] Hägele D, Gestreich M, Rühle W W, Nestle N and Ebeil K 1998 *Appl. Phys. Lett.* **73** 1580
[8] Jalil M B A 2005 *J. Appl. Phys.* **97** 024507
[9] Schmidt G, Ferrand D, Molenkamp L W, Filip A T and van Wees B J 2000 *Phys. Rev.* B **62** R4790
[10] Monzon F G and Roukes M L 1999 *J. Magn. Magn. Mater.* **632** 198
[11] Perel' V I, Tarasenko S A, Yassievich I N, Ganichev S D, Bel'kov V V and Prettl W 2003 *Phys. Rev.* B **67** 201304(R)
[12] Koga T, Nitta J, Takayanagi H and Datta S 2002 *Phys. Rev. Lett.* **88** 126601
[13] Sakurai J J 1994 *Modern Quantum Mechanics* (Reading, MA: Addison-Wesley)
[14] Gasiorowicz S 1996 *Quantum Physics* 2nd edn (New York: Wiley)
[15] Tarasenko S A, Perel' V I and Yassievich I N 2004 *Phys. Rev. Lett.* **93** 056601
[16] Ting D Z-Y and Cartoixà X 2003 *Phys. Rev.* B **68** 235320
[17] Voskoboynikov A, Liu S S, Lee C P and Tretyak O 2000 *J. Appl. Phys.* **87** 387
[18] de Sousa R and Sarma S D 2003 *Phys. Rev.* B **68** 155330
[19] Tan S G, Jalil M B A, Liew T, Teo K L and Chong T C 2005 *J. Appl. Phys.* **97** 10D506
[20] Romo R and Ulloa S E 2005 *Phys. Rev.* B **72** 121305(R)
[21] Nitta J, Akazaki T, Takayanagi H and Enoki T 1997 *Phys. Rev. Lett.* **78** 1335
[22] Bandyopadhyay S and Cahay M 2004 *Appl. Phys. Lett.* **85** 1433
[23] Mal'shukov A G, Tang C S, Chu C S and Chao K A 2005 *Phys. Rev. Lett.* **95** 107203
[24] Jiang L and Wu M W 2005 *Phys. Rev.* B **72** 033311